J. Mater. Chem. 6(3), 469-477 (1996).

Consumption of SiC whiskers by the Al–SiC reaction in aluminium-matrix SiC whisker composites

Shy-Wen Lai and D. D. L. Chung*
Composite Materials Research Laboratory, State University of New York at Buffalo, Buffalo, NY 142600-4400, USA

The Al–SiC reaction in aluminium-matrix SiC composites made by liquid metal infiltration resulted in the formation of silicon, the amount of which increased with increasing SiC volume fraction, but the fraction of SiC consumed by the reaction increased with decreasing SiC volume fraction. For SiC whisker composites made at an infiltration temperature of 800 °C, the fraction of SiC consumed was 18, 26 and 55% at SiC volume fractions of 0.31, 0.23 and 0.10, respectively. The fraction of SiC whiskers consumed was inversely proportional to the volume fraction of SiC whiskers in the composite. The product of these two fractions provides a scale (called the reactivity index) that describes the Al–SiC reactivity. The index decreased with decreasing infiltration temperature and was higher for SiC whiskers than SiC particles. Even at an infiltration temperature of 670 °C, the fraction of SiC whiskers consumed was 26% at an SiC volume fraction of 0.10. In contrast, the fraction of SiC consumed was only 8.4% for a 55 vol.% SiC particle composite made at an infiltration temperature of 800 °C. The fractional consumption values were obtained by determining the silicon concentration in the aluminium matrix *via* calorimetric measurement of the liquidus–eutectic temperature difference.

Silicon carbide (SiC) is the most commonly used filler in aluminium for obtaining composites of high strength, high modulus and low density. Both particle and whisker forms of SiC are used for this purpose. Aluminium is the most commonly used metal matrix material because of its low density and low melting temperature, which makes composite fabrication by liquid metal infiltration and stir casting economical.

The reactivity between SiC and Al is well known:[1–10]

$$4Al + 3SiC \rightarrow Al_4C_3 + 3Si$$

This reaction is detrimental to the strength of the filler–matrix interface, as Al_4C_3 is brittle.[6,8] Moreover, it is detrimental to the filler, as SiC is consumed by the reaction.[4] The reaction is only significant at elevated temperatures, which are encountered during composite fabrication by liquid metal infiltration or stir casting, or during remelting after composite fabrication. The reaction may be greatly diminished by using Al–Si with more than 7 mass% Si as the matrix,[5] but the low ductility of Si-containing Al matrices causes the composite to be low in strength compared with the corresponding composite with pure Al as the matrix.[11]

Although there have been numerous studies on the Al–SiC reaction, relatively little work has been reported on the fraction of SiC consumed by the reaction; the only such report was made by Lloyd and Jin,[4] whose study was limited to a composite (with 6061 as the Al matrix) containing 20 vol.% SiC particles. They reported that the fraction of SiC consumed was 0% after composite fabrication by stir casting and subsequent extrusion, and ≥20% after subsequent remelting at >675 °C for 1 h. Open questions that remain pertaining to the fraction of SiC consumed include: (1) how does the SiC volume fraction affect the fraction of SiC consumed?; (2) how does the fraction of SiC consumed differ between SiC whiskers and SiC particles?; and (3) what is the fraction of SiC consumed in the case of composites fabricated by liquid metal infiltration instead of stir casting?

The objective of this paper was to answer these questions.

Experimental

Composite fabrication

SiC particles and whiskers were used as the reinforcement. The SiC particles used were kindly provided by Electro Abrasives, Corp. (Buffalo, NY, USA) (no. 1200-W). The SiC particle size ranged from 1 to 10 μm, with a mean size of 3 μm. The SiC whiskers used were obtained from Advanced Refractory Technologies, Inc. (Buffalo, NY, USA). The properties of the SiC powder and whiskers are listed in Table 1. The composition of the SiC powder was found to be: 98.5% SiC, 0.5% SiO_2, 0.3% Si, 0.08% Fe, 0.1% Al, 0.3% C; that of the SiC whiskers was: 99% SiC, 0.4% SiO_2 and 0.6% trace metal impurities.

The metal used was aluminium (170.1), the tensile strength of which was 65 MPa. Its composition was Al (99.77%), Fe (0.16%) and Si (0.07%) and its melting temperature was 660 °C.

The metal-matrix composites were fabricated by vacuum infiltration of a liquid metal into a porous preform under an argon pressure. The preform was a green body comprising SiC powder or whiskers. During composite fabrication, the preform was placed at the bottom of a graphite mould. Above the preform was placed a ceramic cloth layer and then an aluminium ingot. The ceramic cloth was used to prevent contact between the SiC preform and the aluminium melt before the infiltration pressure was applied. The fabrication parameters were explained in detail in previous papers.[10,11] In general, the infiltration temperature was 800 °C, while the infiltration pressure was 2000 psi (13.8 MPa) for Al/SiC whisker composites and 6000 psi (41.4 MPa) for Al/SiC particle composites. With all other parameters unchanged, the minimum infiltration pressure increased with increasing volume fraction of the reinforcement. In the case of Al/SiC composites containing

Table 1 Properties of SiC particles and whiskers

	particles	whiskers
mean diameter/μm	3.0	1.4
mean length/μm	—	18.6
density/g cm^{-3}	3.18	3.21
Young's modulus/GPa	400–440	400–440
thermal conductivity/ W m^{-1} K^{-1}	90	—
coefficient of thermal expansion/10^6 °C^{-1}	3.4	—
crystal structure	hexagonal (α)	cubic (β)
SiC (mass%)	98.5	99
SiO_2 (mass%)	0.5	0.4

10 vol.% whiskers, the effect of the infiltration pressure on the degree of infiltration was studied. As shown in Table 2, at an infiltration pressure of 45 psi (0.3 MPa), no liquid metal infiltration occurred. With the infiltration pressure increased to 200 psi (1.4 MPa), the infiltration occurred completely (with less than 5% porosity in the resulting composites). A porosity of less than 0.5% was achieved by further increasing the pressure to 800 psi (5.5 MPa).

The SiC preforms were prepared by wet casting, which involved compressing in a die a slurry containing SiC powder or whiskers, a liquid carrier (acetone) and a binder (an acid phosphate formed from aluminium hydroxide and phosphoric acid.[12–14]) For particulate preforms, the carrier:binder ratio was from 40:1 to 45:1 by volume, as this amount of binder was sufficient to maintain rigidity in the preform. Excessive amounts of binder caused the particulate preform to be not porous enough for subsequent liquid metal infiltration, even at 6000 psi (41.4 MPa). For whisker preforms (which have lower filler-volume fractions), the amount of binder in the preform was greater, corresponding to a carrier:binder ratio of 15:1. The die allowed any excessive liquid to be squeezed out. After removal from the die, the compact was dried in a fume hood at room temperature for 3 h. After drying, which removed most of the acetone, the preform was fired by (i) placing the preform in a furnace at room temperature, (ii) heating to 510 °C at a controlled rate of 1.4 °C min^{-1}, (iii) holding at 510 °C for 3 h, and (iv) cooling in the closed furnace. Ref. 10, 12–14 give the phases formed in the preform due to the binder after heating the SiC particle and whisker preforms, respectively, at different temperatures. The binder content was *ca.* 0.1 mass% of the particle preform[10] and *ca.* 5 mass% of the whisker preform.[13] Excessive heating and a non-uniform temperature distribution in the furnace had to be avoided, as they would cause quick evolution of acetone and thermal stresses, thus resulting in cracking during the firing. The preforms were cylinders, 4.00 cm in diameter, with a height-to-diameter ratio of 0.5, for all the composites used in this study. In this paper, 'composite cylinder' refers to the metal infiltrated cylindrical preform and 'excess aluminium' refers to the metal cast around the preform during infiltration. The pressure used during compression of the slurry was adjusted to vary the SiC volume fraction in the resulting preform.

Table 2 Effect of the infiltration pressure on the degree of infiltration for the Al/SiC composite containing 10 vol.% whiskers

infiltration pressure /psi	/MPa	degree of infiltration	porosity (%)
45	0.3	none	—
200	1.4	complete	<5
800	5.5	complete	<2
2000	13.8	complete	<0.5

Composite characterization

Metallography. Fig. 1(a) and (b) show SEM images of the Al/SiC composite cylinders containing 10 vol.% whiskers, which were fabricated with an infiltration pressure of 200 psi (1.4 MPa) and 2000 psi (13.8 MPa), respectively. The porosity (*ca.* 5%) was clearly observed for the Al/SiC fabricated at 200 psi (1.4 MPa). The porosity was diminished by increasing the infiltration pressure to 2000 psi (13.8 MPa). Fig. 1(c) shows that, at an infiltration pressure of 2000 psi (13.8 MPa), the Al/SiC composite containing 31 vol.% SiC whiskers exhibited *ca.* 3% porosity. This indicates that the infiltration pressure should be increased with increasing volume fraction of SiC whiskers in order for complete infiltration to occur. Fig. 2 shows SEM photographs of both the excess aluminium and the edge regions of Al/SiC composite cylinders containing 10 and 23 vol.% whisker reinforcement. The presence of needle-shaped Si precipitates in the excess Al regions [Fig. 2(b) and (d)] indicated that the Al–SiC reaction occurred in both composites. The higher concentration of the Si precipitates for the 23 vol.% SiC whisker composite than the 10 vol.% SiC whisker composite indicates that the extent of Al–SiC reaction was larger at the higher SiC whisker volume fraction. Both composites contained uniformly distributed SiC whiskers and are expected to have isotropic properties. Note that the Al/SiC composite containing 23 vol.% SiC whiskers shows a slightly higher porosity compared to the Al/SiC composite containing 10 vol.% SiC. A similar morphology of Si precipitates in the form of eutectic Al–Si was observed (not shown) between the primary Al dendrites in the excess aluminium around Al/SiC containing 55 vol.% SiC particles. This indicates that Si, a product of the Al–SiC reaction, diffused outward to the excess aluminium and formed a hypoeutectic Al–Si alloy. The amount of Si in the excess aluminium increased with increasing volume fraction of reinforcement in the Al/SiC. This also indicates that the SiC whiskers, though in a single crystal form, reacted with aluminium at high temperatures (during infiltration), just as the SiC particles (not single crystals) did.

No Al–Si eutectic or dendritic morphology was microscopically observed within the Al/SiC composite cylinders containing either SiC particles or SiC whiskers. This negative observation may be due to the very small SiC filler spacing in the Al/SiC composite. In order to study the location of Si (reaction product) in Al/SiC, the Al/SiC particulate composite

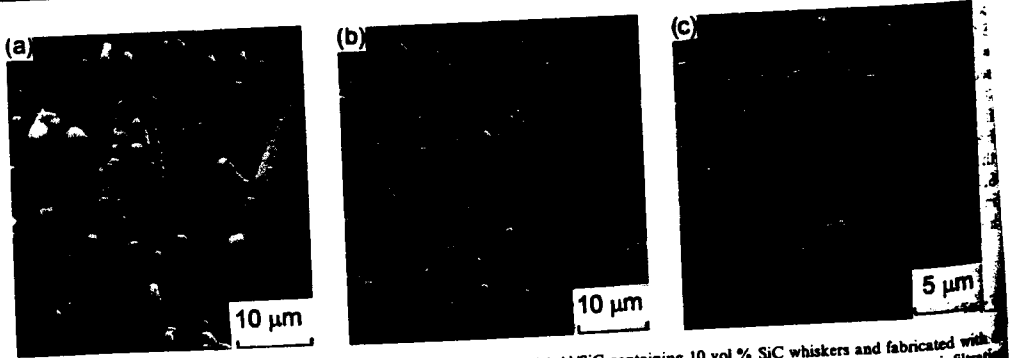

Fig. 1 SEM photographs of polished sections of various Al/SiC composites. (a) Al/SiC containing 10 vol.% SiC whiskers and fabricated with an infiltration pressure of 200 psi (1.4 MPa). Porosity *ca.* 5%. (b) Al/SiC containing 10 vol.% SiC whiskers and fabricated with an infiltration pressure of 2000 psi (13.8 MPa). Porosity <0.5 %. (c) Al/SiC containing 31 vol.% SiC whiskers and fabricated with an infiltration pressure of 2000 psi (13.8 MPa). Porosity *ca.* 3%.

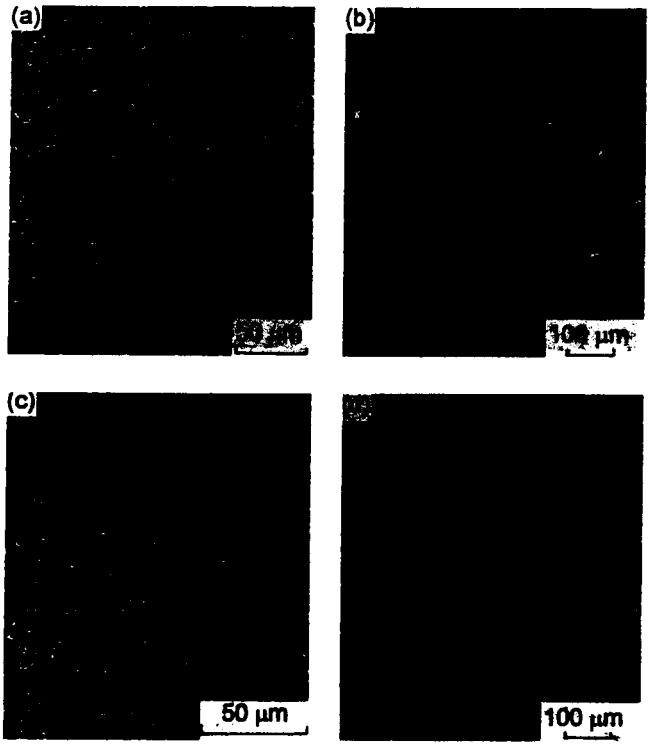

Fig. 2 SEM photographs of polished sections of Al/SiC whisker composites. (a) 10 vol.% SiC whisker composite. (b) The excess aluminium surrounding the 10 vol.% SiC whisker composite cylinder. (c) 23 vol.% SiC whisker composite. (d) The excess aluminium surrounding the 23 vol.% SiC whisker composite cylinder.

55 vol.% particles) was etched with acids to completely remove the aluminium. Unlike the preform which showed clean isolated SiC particles (not shown), Fig. 3(a) shows that the SiC particles were connected to form a network. Fig. 3(b) shows an SEM image at a higher magnification, which shows that Si precipitated between adjacent SiC particles, thereby forming a network. Similarly, Fig. 4 shows the SEM morphology of plain SiC whiskers and a fully etched Al/SiC whisker composite containing 23 vol.% whiskers. Unlike the clear morphology in plain SiC whiskers [Fig. 4(a) and (c)], the SiC whiskers in the etched composite were connected by the Si precipitates [Fig. 4(b) and (d)]. Although not confirmed statistically, the SiC whiskers in the Al/SiC composites tended to have a smoother and rounder surface morphology compared with plain SiC whiskers. This may be due to the Al–SiC reaction at the ends and surface of the SiC whiskers during composite fabrication.

X-Ray diffraction. X-Ray diffraction (XRD) was performed with Cu-Kα radiation in different regions of the Al/SiC particle composite cylinder in order to investigate the phase distribution. We had previously studied the non-uniform phase (Si,

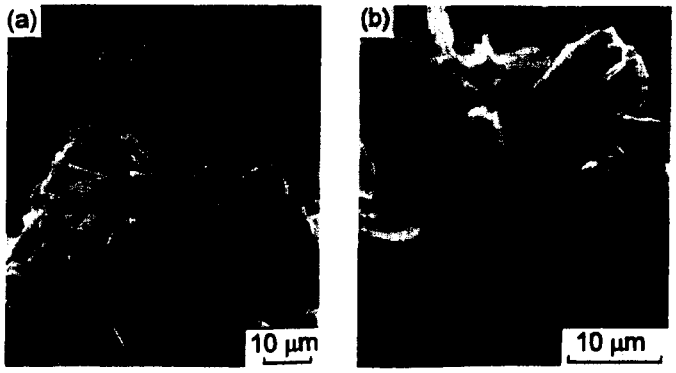

SEM photographs of a fully etched Al/SiC composite containing 55 vol.% SiC particles. Si precipitated and bridged adjacent SiC particles.

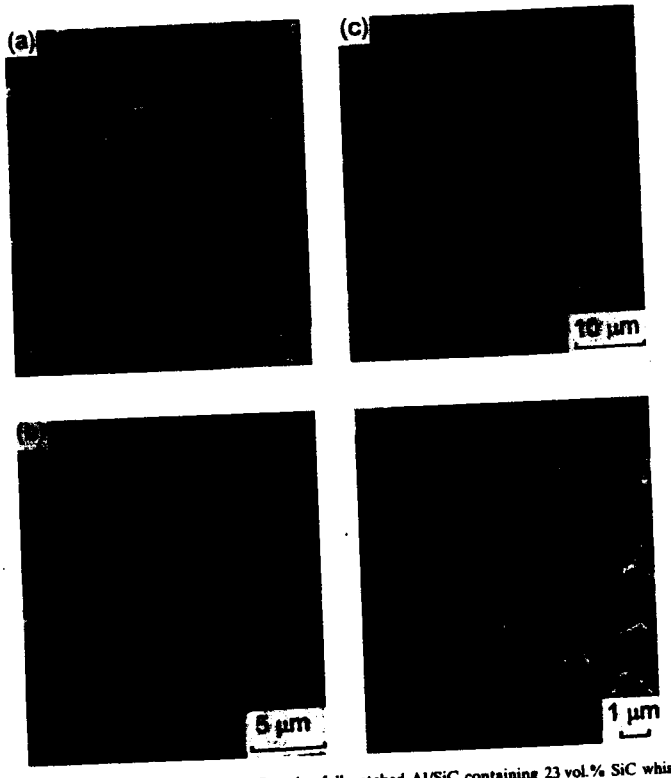

Fig. 4 SEM photographs of plain SiC whiskers [(a) and (b)] and a fully etched Al/SiC containing 23 vol.% SiC whiskers [(c) and (d)]. (a) and (b) show clear whisker surface morphology; (c) and (d) show that Si precipitated and bridged adjacent SiC whiskers.

SiC and Al_4C_3) distributions throughout the Al/SiC particle composite cylinder.[10] For details of the experimental procedures and notations of the locations within the composite cylinder, see ref. 10. Fig. 5 shows the XRD patterns of the excess aluminium and the edge region of the Al/SiC particle composite cylinder. Only Al and Si peaks were present in the excess aluminium surrounding the composite cylinder. No Al_4C_3 peak was found in the excess aluminium, even though this region was next to the graphite mould. However, in the edge region of the composite cylinder, Al_4C_3 peaks were weakly present, due to the reaction between SiC and Al. In order to investigate the silicon distribution, all Al/SiC particulate and whisker composites were fully etched using an acid solution of HCl, H_2SO_4 and distilled water (1:1:5). The acid solution leached away Al_4C_3 and Al, but not SiC and Si. Fig. 6 shows the XRD patterns of the Al/SiC whisker composites containing 10 and 31 vol.% SiC whiskers and 55 vol.% SiC particles. The Al/SiC composite containing 10 vol.% SiC whiskers exhibited

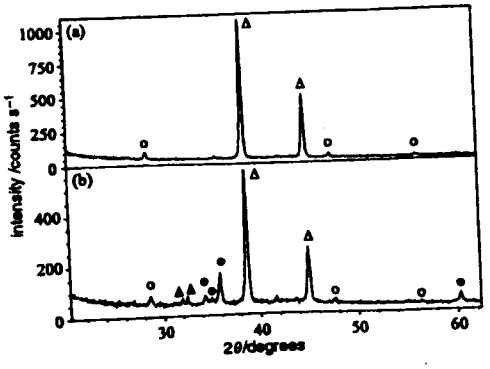

Fig. 5 Powder XRD patterns of (a) the excess aluminium and (b) the edge region of Al/SiC containing 55 vol.% SiC particles. ●, SiC; ○, Si; △, Al; ▲, Al_4C_3.

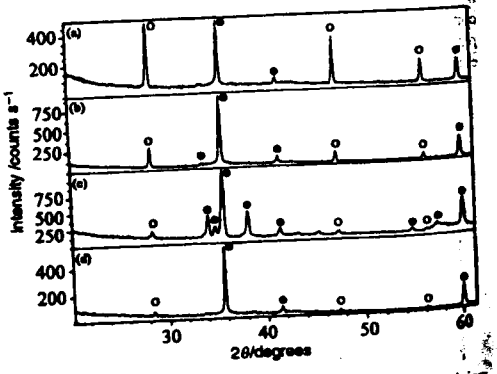

Fig. 6 Powder XRD patterns of various Al/SiC composites containing (a) 10 vol.% SiC whiskers, (b) 31 vol.% SiC whiskers, (c) 55 vol.% SiC particles; and (d) 10 vol.% SiC whiskers. The composite of (d) was made at an infiltration temperature of 670 °C. The composites of (a), (b) and (c) were made at an infiltration temperature of 800 °C. The patterns were taken from the centre of the bottom face of the composite cylinder. ●, SiC; ○, Si.

larger Si peaks relative to the SiC peaks [Fig. 6(a)] than the Al/SiC whisker composite containing 31 vol.% whiskers [Fig. 6(b)]. This indicates that more SiC whiskers were consumed due to the Al–SiC reaction in the Al/SiC whisker composite containing less whiskers. Fig. 7 shows the Si:SiC intensity ratio in the bottom slice of each of the Al/SiC composite cylinders containing 10 and 31 vol.% SiC whiskers and 55 vol.% particles. All three composites exhibited a trend of increasing Si:SiC intensity ratio as the distance from the edge of the composite cylinder increased. In agreement with ref. 10, this means that the silicon, an Al–SiC reaction product, diffused outward to the excess aluminium during composite fabrication for all three composites. The Si out-diffusion occurred for both whisker and particulate Al/SiC composites.

In order to investigate the actual Si content in the matrix of Al/SiC composites, two kinds of Si powder were mixed with either the SiC whiskers or SiC particles at various atomic Si:SiC ratios for XRD. One kind of Si was amorphous Si powder (Sicomill UN1346), which was obtained from KemaNord Industrikemi (Ljungaverk, Sweden). Although it was rated amorphous, clear Si XRD peaks were found. The other kind of Si powder was obtained by grinding a 99.9999% pure polycrystalline Si lump, which was obtained from Fisher Scientific Co. (Pittsburgh, PA, USA). Fig. 8 shows that the mixtures involving either SiC particles or SiC whiskers separately gave linear relationships between the Si:SiC X-ray intensity ratio and the atomic Si:SiC ratio. The two kinds of Si powder gave consistent results. For the SiC particles, the slope of the plot of the Si:SiC X-ray intensity ratio against the Si:SiC atomic ratio was 2.2795, which was obtained by the least-squares method. For the SiC whiskers, the slope of the plot of the Si:SiC X-ray intensity ratio against the Si:SiC atomic ratio was 1.0604. Table 3 shows the Si content (in mass%) in the matrix of Al/SiC (bottom slice of the composite cylinder), as obtained from XRD results and the conversion provided by Fig. 8. The Si content in the matrix of Al/SiC increased with increasing distance from the edge of the composite cylinder, whether SiC whiskers or particles were used. The Si content in the matrix also increased with increasing volume fraction of SiC at each corresponding location of the composite cylinder. The highest Si content of 8.60 mass% was observed in the centre (20 mm from the edge) of the Al/SiC particulate composite containing 55 vol.% SiC particles. Even this highest Si content was below the Si content of the Al–Si eutectic (12 mass%). Since the Si:SiC intensity ratio varied

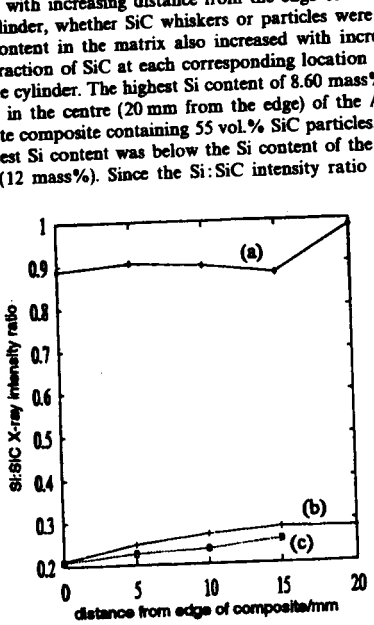

Si:SiC integrated intensity ratio (from XRD) as a function of distance from the cylindrical edge of: (a) Al/SiC containing .% SiC whiskers; (b) Al/SiC containing 31 vol.% SiC whiskers; (c) Al/SiC containing 55 vol.% SiC particles. The results were ed from the bottom slice of each composite.

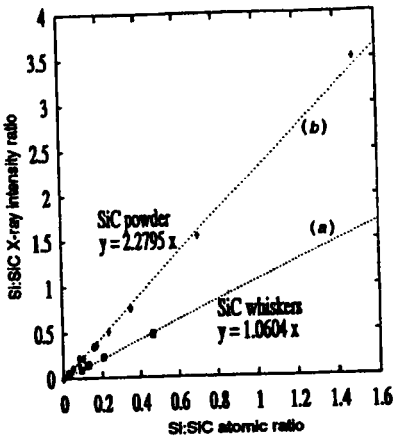

Fig. 8 Linear relationship of the Si:SiC X-ray intensity ratio and the Si:SiC atomic ratio for (*a*) SiC whiskers ($y = 1.0604x$), and (*b*) SiC particles ($y = 2.279x$). ◇/□, Si powder A; +, Si powder B.

Table 3 Comparison of the Si content (in mass%) obtained by XRD and DSC in the Al matrix of Al/SiC (bottom slice) at each corresponding location

SiC volume fraction	experimental method	distance from the edge of the composite cylinder/mm				
		0	5	10	15	20
0.10[a]	XRD	4.42	4.46	4.43	4.39	4.66
	DSC	4.62	4.90	4.83	5.04	5.06
0.31[a]	XRD	4.45	5.07	5.27	5.66	5.63
	DSC	5.78	6.10	6.42	6.67	6.85
0.55[b]	XRD	8.52	9.21	9.51	10.3	—
	DSC	6.32	6.72	7.23	8.18	8.60

[a] SiC whiskers. [b] SiC particles.

throughout the composite cylinder, the value at the centre of the bottom slice was used to investigate the effect of the reinforcement amount on the extent of the Al–SiC reaction (the Si content in the matrix indicates the extent of the Al–SiC reaction. The Al–SiC reaction rate is expected to decrease with increasing extent of infiltration, as the aluminium matrix contains more Si as infiltration proceeds, thereby causing further Al–SiC reaction to diminish[5]).

The extent of the Al–SiC reaction is expected to decrease with decreasing infiltration temperature. Fig. 6(d) shows the XRD pattern of the Al/SiC composite containing 10 vol.% SiC whiskers, which was fabricated at the infiltration temperature of 670 °C. A low Si peak intensity indicates that the Al–SiC reaction occurred only slightly at this infiltration temperature. However, it had been shown in a previous study[10] that incomplete infiltration occurred at the infiltration temperature of 670 °C for Al/SiC containing a high volume fraction of reinforcement. The required infiltration temperature and pressure are expected to increase with increasing volume fraction of the reinforcement.

Although the XRD technique can be used for the investigation of phase distributions, this work is focused on the use of differential scanning calorimetry (DSC) to study the Si concentration variation throughout the Al/SiC particle or whisker composites, since DSC requires no sample etching and thus can provide more accurate composition analysis.

Differential scanning calorimetry. A Perkin-Elmer differential scanning calorimeter (DSC 7) was used to measure the melting

temperatures and the associated enthalpy changes of the phases or microconstituents in the matrix of the Al/SiC composite and in the excess aluminium around the composite cylinder.

Fig. 9(a) shows DSC thermograms of the Al/SiC composite which contained 10 vol.% SiC whiskers and was fabricated at the infiltration temperature of 670 °C. The thermograms were obtained on cooling from 700 to 500 °C at a cooling rate of 10 °C min^{-1} for three local regions in the bottom slice (1 mm thick) of the composite cylinder. The three local regions were A (the excess aluminium adjacent to the edge of the composite, within 1 mm from the edge), B (the edge of the slice, within 1 mm from the cylindrical edge, such that the region was within the composite) and C (the centre of the slice, within 0.5 mm from the centre). Region A gave an exothermic peak (the liquidus) with its onset at 655 °C and a small solidus peak at about 630 °C. Regions B and C exhibited exothermic peaks (liquidus) with similar onsets at about 637 °C and exothermic peaks (eutectic) with onsets at about 570 °C. This indicates that, even at the infiltration temperature of 670 °C, the silicon content (due to the Al–SiC reaction) in the aluminium matrix of the composite is greater than the silicon solubility (1.6 mass%) in the aluminium. Both the edge and centre regions exhibited similar temperature differences (ΔT) between the liquidus and the eutectic, indicating that both regions had similar silicon contents in the aluminium matrix. This also indicates the absence of a non-uniform Si phase distribution in Al/SiC containing 10 vol.% whiskers and fabricated at the infiltration temperature of 670 °C.

Fig. 9(b) shows DSC thermograms of the Al/SiC composite which contained 23 vol.% SiC whiskers and was fabricated at the infiltration temperature of 800 °C. The thermograms were obtained on cooling from 700 to 500 °C at a cooling rate of 10 °C min^{-1} for four local regions in the bottom slice (1 mm thick) of the composite cylinder. The four local regions were A (the excess aluminium adjacent to the edge of the composite, within 1 mm from the edge), B (the edge of the slice, within 1 mm from the cylindrical edge, such that the region was within the composite), C (the half radius of the slice, within 0.5 mm from the centre) and D (the centre of the slice, within 0.5 mm from the centre). Region A exhibited exothermic peaks with onsets at 570.5 and 625.8 °C; region B exhibited exothermic peaks with onsets at 570.1 and 615.0 °C; region C exhibited exothermic peaks with onsets at 570.6 and 609.2 °C; and region D exhibited exothermic peaks with onsets at 570.1 and 607.6 °C. The first peak for each region *i.e.*, the one at 570–571 °C, is attributed to the Al–Si eutectic invariant reaction at 577 °C. The second peak for each region is attributed to the liquidus of the Al–Si alloy matrix. No other peak was observed in all regions, indicating no contamination associated with the matrix–mould reaction.

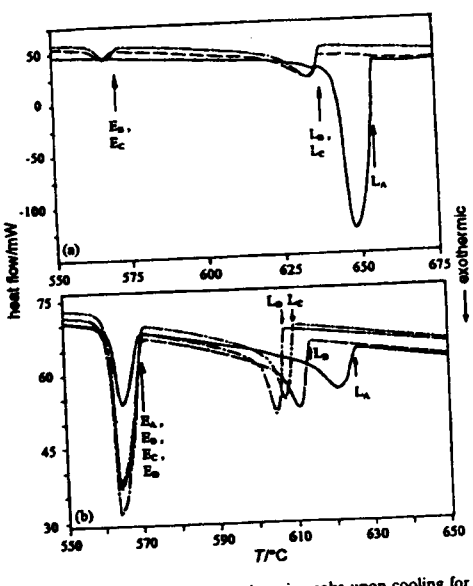

Fig. 9 (a) DSC scans showing exothermic peaks upon cooling for the Al/SiC composite containing 10 vol.% SiC whiskers and made at an infiltration temperature of 670 °C. A, excess aluminium adjacent to the edge of the composite cylinder; B, edge of bottom slice within composite; C, centre of bottom slice of composite cylinder; L = liquidus; E = eutectic. (b) DSC scans showing exothermic peaks upon cooling for the Al/SiC composite containing 23 vol.% SiC whiskers and made at an infiltration temperature of 800 °C. A, excess aluminium adjacent to edge of composite cylinder; B, edge of bottom slice within composite; C, mid-radius region of bottom slice of composite cylinder; D, centre of bottom slice of composite cylinder; L = liquidus; E = eutectic.

The temperature difference (ΔT) between the first DSC peak (corresponding to the solidus or the eutectic temperature) and the second DSC peak (corresponding to the liquidus) was used to evaluate the Si content in each region of the composite. The ΔT values were 55.3, 44.8, 38.3 and 36.4 °C for regions A, B, C and D, respectively, of the Al/SiC whisker (23 vol.% whiskers) composite [Fig. 9(b)]. The Al/SiC composite which contained 10 vol.% whiskers and was fabricated at 800 °C exhibited a similar trend in that ΔT decreased with increasing distance from the edge to the centre of the composite. As shown in Table 4, ΔT decreased with increasing distance from the edge to the centre of the composite cylinder for all composites except for the Al/SiC whisker composite fabricated at the infiltration temperature of 670 °C. This means that the Si content in the aluminium matrix (obtained from ΔT based on the Al–Si phase diagram) increased from the edge to the centre, as shown in Table 3, which also shows good agreement between the Si content based on DSC and that based on XRD. The Si amount (based on ΔT) at each corresponding position in the aluminium matrix increased with increasing volume fraction of the reinforcement (Fig. 10). The severity of the non-uniform Si phase distribution (*i.e.*, the average slope of Si variation along the line from the edge to the centre) also increased with increasing volume fraction of the reinforcement.

Based on the approach outlined in ref. 4, the relative amount of SiC which was consumed by the Al–SiC reaction was obtained. Table 5 shows the percentage of SiC consumed (based on DSC results) for Al/SiC particulate and whisker composites fabricated at the infiltration temperature of 800 °C (with various SiC volume fractions) at the centre region of the bottom slice of each composite. The lower the volume fraction of the SiC reinforcement, the higher the fraction of SiC consumed for a given infiltration temperature. The Al–SiC reaction is detrimental to the tensile properties of Al/SiC because of the decrease of the strength of the SiC reinforcement due to the Al–SiC reaction and the brittle interfacial reaction products. The most severe SiC consumption occurred for the Al/SiC containing 10 vol.% SiC whiskers, as 55 vol.% of the SiC reacted with aluminium. Upon decreasing the infiltration temperature to 670 °C, the SiC consumption was reduced to 26%.

Scratch/shear testing. For interfacial shear strength testing, the shear/scratch test was performed with a Teledyne Taber Model 139 shear/scratch tester, which was equipped with a Taber S-20 contour tungsten carbide shear tool. The applied load on the tool was 1000 g. One or two scratches were made on the specimen surface for each increment of 5 mm from the cylindrical edge of the composite; the more uniform scratch (groove) was used for the determination of the scratch width with the help of a 10× magnifier. The larger the scratch width the lower was the shear strength.

Table 6 shows the scratch width of Al/SiC composites

Table 4 Liquidus–solidus temperature difference (ΔT, from DSC) and Si content (mass%, from XRD) in the Al matrix of Al/SiC (bottom section) fabricated with a graphite mould at the infiltration temperature of 780 °C

SiC volume fraction	infiltration temperature/°C		distance from the edge of the composite cylinder/mm				
			0	5	10	15	20
0.10[a]	670	Si (mass%)	2.23	—	—	—	2.39
		ΔT	66.9	—	—	—	65.7
0.10[a]	800	Si (mass%)	4.62	4.90	4.83	5.04	5.06
		ΔT	49.8	47.8	48.3	46.8	46.7
0.23[a]	800	Si (mass%)	5.32	6.15	6.23	6.25	6.50
		ΔT	44.8	38.9	38.3	38.2	36.4
0.31[a]	800	Si (mass%)	5.78	6.10	6.42	6.67	6.85
		ΔT	41.5	39.3	37.0	35.2	33.9
0.55[b]	670	Si (mass%)	3.26	3.86	3.92	[c]	[c]
		ΔT	59.5	55.2	54.8	[c]	[c]
0.55[b]	800	Si (mass%)	6.32	6.72	7.23	8.18	8.60
		ΔT	37.7	34.8	31.2	24.4	21.4

[a] SiC whiskers. [b] SiC particles. [c] Incomplete infiltration region.

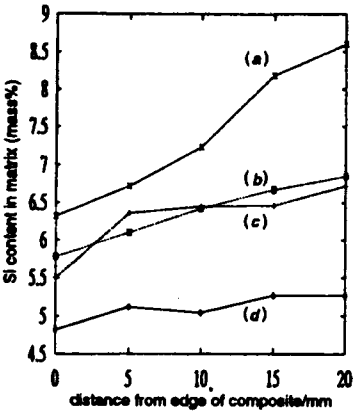

Fig. 10 Silicon content (mass%, obtained from DSC) in the aluminium matrix of various Al/SiC composites as a function of distance from the composite cylindrical edge. (*a*) Al/SiC_p, 55 vol.%; (*b*) Al/SiC_w, 31 vol.%; (*c*) Al/SiC_w, 23 vol.%; (*d*) Al/SiC_w, 10 vol.% p = particles; w = whiskers.

various reinforcement volume fractions. The scratch width decreased with increasing volume fraction of the reinforcement, indicating that the shear strength of Al/SiC increased due to the addition of SiC particles or whiskers. Negligible shear strength variation was observed within each composite, in spite of the observed variation in Si content (Table 3). This indicates that a non-uniform Si distribution did not cause a non-uniform shear strength distribution, as reported in ref. 10.

Tensile testing. Tensile testing was performed using a hydraulic Mechanical Testing System (MTS) with a loading rate of 120 lb min^{-1} (534 N min^{-1}) at room temperature. Samples in the shape of a dogbone were machined from the composite cylinder, with the dogbone axis perpendicular to the axis of the composite cylinder, so the mechanical properties measured were those near the centre of the composite cylinder. Young's modulus was measured using a strain gauge at low loads. The ductility was determined by drawing two parallel lines marking the gauge length on the sample and measuring the distance between the lines before and after tensile testing using calipers.

Table 7 lists the tensile properties of Al/SiC whisker composites. The yield strength, ultimate strength and modulus increased while the ductility decreased with increasing SiC whisker volume fraction at the same infiltration temperature

Table 5 Silicon content (mass%) in the aluminium matrix (in the bottom centre region) and the percentage of the SiC consumed due to the Al–SiC reaction

SiC volume fraction	SiC mass fraction	Si content in composite (mass%)[d]	Si content in Al matrix (mass%)	fraction of SiC consumed (%)	reactivity index[e]
0.10[a,b]	0.117	8.17	2.39	25.8	0.0258
0.10[a]	0.117	8.17	5.06	54.7	0.0547
0.23[a]	0.262	18.35	6.50	25.9	0.0596
0.31[a]	0.348	24.37	6.85	18.3	0.0567
0.55[b]	0.592	41.44	8.60	8.4	0.0462

[a] SiC whiskers. [b] Infiltration temperature = 670 °C for this composite and 800 °C for the other four composites in this table. [c] SiC particles. [d] This refers to Si in SiC. [e] Product of the fraction SiC consumed and the original SiC volume fraction.

Table 6 Scratch width (mm) of Al/SiC particulate and whisker composites (standard deviation in parentheses)

SiC volume fraction	Distance from the edge of the composite cylinder/mm				
	0	5	10	15	20
0.10[a]	0.99(0.02)	1.01	0.97	0.97	0.97
0.23[a]	0.80	0.75	0.80	0.80	0.80
0.55[b]	0.59(0.02)	0.59(0.01)	0.58(0.02)	0.56(0.04)	0.56

[a] whiskers. [b] SiC particles.

Table 7 Tensile properties of Al/SiC whisker composites fabricated at an infiltration pressure of 2000 psi (standard deviations based on three samples of each type in parentheses)

SiC volume fraction	infiltration temperature/°C	yield strength/MPa	ultimate strength/MPa	modulus/GPa	ductility (%)
0.10	670	108.7(8.6)	224.1(5.4)	93.0(10.2)	7.8(0.5)
0.10	800	105.7(3.6)	181.3(8.6)	97.6(19.1)	2.6(1.5)
0.23	800	156.6(7.6)	282.1(5.9)	106.7(10.5)	2.4(1.2)
0.31	800	204.4(39.2)	309.7(16.3)	150.4	1.0

of 800 °C. A decrease in the infiltration temperature from 800 to 670 °C increased the ultimate strength and ductility (as expected from the decreased fraction of SiC consumed), whilst having little effect on yield strength or modulus.

The composite yield strength (σ_{cy}) was calculated by using eqn (1):[15]

$$\sigma_{cy} = \sigma_{my}\,[V_m(S+2)/2 + V_m] \quad (1)$$

where σ_{my} is the matrix yield strength (65 MPa), S is the whisker aspect ratio (13.3 before composite fabrication) and V_m is the matrix volume fraction. If the SiC consumption caused the whisker diameter to decrease without affecting the whisker length, the aspect ratio would increase from 13.3 to the modified values listed in Table 8. Furthermore, the SiC consumption caused the whisker volume fraction to decrease to the modified values listed in Table 8. The yield strength calculated using the original whisker volume fraction and the original whisker aspect ratio, and the yield strength calculated using the modified whisker volume fraction and the modified whisker aspect ratio were both quite close to the corresponding measured yield strength (Table 8). The increase of the SiC whisker aspect ratio and the decrease of the whisker volume fraction, both caused by the Al–SiC reaction, affected the yield strength in opposite directions, so that the yield strength appeared unaffected by the Al–SiC reaction. As a result, eqn. (1) gave good theoretical fits to the measured yield strength, whether or not the effects of the Al–SiC reaction on the whisker aspect ratio and volume fraction were considered. On the other hand, the ultimate strength is expected to be more affected by the interfacial reaction than the yield strength, but theoretical models for the ultimate strength are not available for the case of discontinuous fibres or whiskers that are not oriented.

Discussion

For the same filler (*i.e.*, SiC whiskers) and the same infiltration temperature, the fraction of SiC consumed increases with decreasing value of the original SiC volume fraction in the composite, as shown in Table 5. These two fractions are in fact inversely proportional to one another, as shown in Table 5 by the constancy of the product of the two fractions. This product, called the reactivity index, provides a scale that describes the Al–SiC reactivity. This means that the variation of the fraction of SiC consumed with the original SiC volume fraction was governed by geometry (probably the surface area of the whiskers per unit volume of the composite, since the reaction is more severe at the onset and decreases in severity as silicon is formed and enters the aluminium matrix). A decrease of the infiltration temperature decreased the reactivity index, as shown in Table 5 for the case of composites containing 0.10 vol.% of SiC whiskers. The reactivity was lower for SiC particles than SiC whiskers for the same infiltration temperature, in spite of the single-crystal nature of the whiskers. This reactivity difference is attributed to the much larger (by a factor of 6) surface area per unit volume of the composite for the SiC whiskers compared to the SiC particles at the same volume fraction.

Although the Si content was highest in the bottom centre region of the composite cylinder (Tables 3 and 4), the SiC consumption was most severe at the very edge of the composite cylinder.[10] The non-uniform Si distribution was merely a consequence of the out-diffusion of the silicon in the liquid Al–Si state to the aluminium melt surrounding the preform during composite fabrication (Fig. 2 and 3). The fraction of SiC consumed (Table 5) obtained by using the Si content in the bottom centre region of the composite cylinder thus reflects the true Al/SiC reactivity.

Even though the SiC whiskers or particles were partially coated by the binder used in preform preparation and the binder concentration was higher in the SiC whisker preforms than the SiC particle preforms, the reactivity between the SiC whiskers and the Al matrix was higher than that between the SiC particles and the Al matrix. This means that the presence of the binder did not attenuate the reactivity much, if any.

This paper provides the fraction of SiC consumed in Al/SiC composites made by liquid metal infiltration, in contrast to earlier work[4,5] on Al/SiC composites made by stir casting. The non-uniform Si distribution reported here applies to composites made by liquid metal infiltration, but not to those made by stir casting.

The method used in this work for determining the fraction of SiC consumed is essentially the same as that used in ref. 4. However, there are two differences. One difference is that we measured the liquidus-eutectic temperature difference, ΔT, whereas the liquidus temperature alone was measured in ref. 4. The advantage of measuring ΔT is that it avoids the effect of the temperature scanning rate. Another difference is related to the calculation of the fraction of SiC consumed based on the silicon content in the aluminium matrix. The calculation yields the fraction of SiC consumed as the expression used in ref. 4 multiplied by the factor [1−(SiC volume fraction)]. In other

Table 8 Comparison of the measured and calculated values of the yield strength of Al/SiC whisker composites [calculated values based on either the original SiC volume fraction together with the original whisker aspect ratio (13.3), or the modified SiC volume fraction together with the modified whisker aspect ratio]

original SiC volume fraction	infiltration temperature/°C	fraction of SiC consumed (%)	modified SiC volume fraction	modified ratio	yield strength/MPa		
					calculated		measured
					original	modified	
0.10	670	25.8	0.074	15.4	108.2	102.1	108.7(8.6)
0.10	800	54.7	0.045	19.8	108.2	94.2	105.7(3.6)
0.23	800	25.9	0.17	15.4	164.3	150.1	156.6(7.6)
0.31	800	18.3	0.25	14.7	198.9	185.9	204.4(39.2)

words, a factor is missing in ref. 4, so that the values given in ref. 4 must be corrected in order to obtain the correct value.

Ref. 4 reported that the fraction of SiC consumed is 37% (*i.e.*, 29% after the correction) for an SiC particle 6061 Al-matrix composite containing 20 vol.% SiC after remelting at 800 °C for 1 h. In this work, the fraction of SiC consumed was 26% for a SiC whisker composite containing 23 vol.% SiC. Thus, the results of ref. 4 and this work are comparable.

Conclusion

The Al–SiC reaction in Al/SiC composites made by liquid metal infiltration caused the reaction product Si to have a non-uniform distribution in the resulting composite, such that the Si concentration decreased from the centre to the edge of the composite (the edge is the interface between the composite and the excess aluminium cast around the composite). The non-uniformity increased in severity as the SiC whisker volume fraction increased and as the infiltration temperature increased; it was present at a SiC volume fraction of 10% when the infiltration temperature was 800 °C, but was absent when the infiltration temperature was 670 °C. However, the non-uniform Si distribution, if any, did not result in a non-uniform mechanical property distribution.

The amount of reaction product Si increased with increasing SiC volume fraction, but the fraction of SiC consumed by the reaction increased with decreasing original SiC volume fraction, such that the two fractions were inversely proportional to one another. The product of the two fractions provides a scale (called the reactivity index) for describing the Al–SiC reactivity. The reactivity decreased with decreasing infiltration temperature, and was higher for SiC whiskers than SiC particles.

This work was supported by the Advanced Research Projects Agency of the US Department of Defense and the Center for Electronic and Electro-Optic Materials of the State University of New York at Buffalo.

References

1 R. Warren and C-H. Anderson, *Composites*, 1984, **15**, 101.
2 T. A. Chernyshova and A. V. Reborv, *J. Less Common Met.*, 1986, **117**, 203.
3 W. C. Moshier, J. S. Ahearn and D. C. Cooke, *J. Mater. Sci.*, 1987, **22**, 1154.
4 D. J. Lloyd and I. Jin., *Met. Trans. A*, 1988, **19**, 3107.
5 D. J. Lloyd, H. Lagace, A. McLeod and P. L. Morris, *Mater. Sci. Eng. A*, 1989, **107**, 73.
6 T. Iseki, T. Kameda and T. Maruyama, *J. Mater. Sci.*, 1984, **19**, 1692.
7 K. Kannikeswaren and R. Y. Lin, *J. Met.*, 1987, **39**, 17.
8 J. C. Viala, P. Fortier and J. Bouix, *J. Mater. Sci.*, 1990, **25**, 1842.
9 H. Ribes, M. Suery, G. L'Esperance and J. G. Legoux, *Met. Trans. A*, 1990, **21**, 2489.
10 S-W. Lai and D. D. L. Chung, *J. Mater. Sci.*, 1994, **29**, 3128.
11 S-W. Lai and D. D. L. Chung, *J. Mater. Sci.*, 1994, **29**, 2998.
12 J-M. Chiou and D. D. L. Chung, *J. Mater. Sci.*, 1993, **28**, 1435.
13 J-M. Chiou and D. D. L. Chung, *J. Mater. Sci.*, 1993, **28**, 1447.
14 J-M. Chiou and D. D. L. Chung, *J. Mater. Sci.*, 1993, **28**, 1471.
15 V. C. Nardone, *Scripta Metallurgica*, 1987, **21**, 1313.

Paper 5/04195C; *Received* 29*th June*, 1995